HEAD LOSSES CAUSED BY AN ICE COVER ON OPEN CHANNELS

PETER A. LARSEN*, *Member*

(Paper presented at a meeting of the Hydraulics Section, Boston Society of Civil Engineers, on November 2, 1966)

Introduction

The design of open channels in areas with long-lasting cold winters requires consideration of various types of ice problems. One such problem is the effect of an ice cover on head losses. The increase of head losses in, for instance, a hydro-power channel is directly proportional to a reduction in power production. In wintertime the value of the power generated would be generally greater than in the warmer periods of the year. The economical aspect is therefore obvious and the question is: What is the cross sectional channel area that will give optimum economy?

Two types of information are necessary for channel design:

1.) Knowledge of the roughness of the ice cover.

2.) A method of computing the effect of the composite roughness of a given channel, the bottom and ice roughness being known.

Very little can be found in the hydraulic literature about ice roughness. Some authors recommend that the same friction factor be used for the ice cover as for the channel bottom. Others suggest that the ice cover be considered as a hydraulically smooth surface. Of these suggestions the latter might appear to be the more logical, but it will be shown that this assumption is generally too optimistic.

As far as the composite roughness is concerned, a variety of formulas can be found based on different assumptions. As pointed out by Ven Te Chow some of these result in negative friction factors for the ice cover, an illogical result.[1]

The aim of this paper is to develop a rational formula for composite roughness based on the concept of logarithmic velocity distribution, and to report some field data relative to the roughness of the ice cover on two different Swedish power channels. The field data provided a check on the deduced formula.

---

*Associate Professor, Worcester Polytechnic Institute, Worcester, Massachusetts.

1. Chow, Ven Te: Open Channel Hydraulics, 1959.

Formation of Ice Covers

In areas with cold climate, it is generally desirable to have an ice cover on the channels. This prevents the production of so-called frazil ice which generally results in the formation of hanging dams or anchor ice with uncontrollable, high head losses.

An ice cover is known to form in either one of two ways. The one dealt with here is the formation similar to the ice covering on a lake. This type of ice cover can form only when the flow velocity is relatively low- less than 2 fps. Such an ice cover is, however, known to be stable at considerably higher velocities than those at which it can be formed. This is due to the fact that the whole flow pattern is changed when the cover is present. The ice forms a rigid boundary and consequently the flow velocity is zero at the ice surface and the maximum velocity occurs somewhere near mid-depth.

An ice cover may also be built up by floating ice which is transported by the flowing stream and deposited at the edge of an ice cover that has formed in a low velocity zone of the channel. Such an ice cover is known to have a relatively high initial resistance coefficient which tends to decrease with time.[2] However, the roughness of the ice cover considered here has been shown to increase with time.

In an investigation made by the Swedish State Power Board, ice floes were sawn out of the ice cover on two different power plant supply channels. Figures 1 to 6 show the under side of the ice floes. A wavy pattern is apparent with its main direction being perpendicular to the direction of flow. A floe with its orientation perpendicular to the direction of flow did not show a regular wave pattern, although the surface was not smooth. The channel characteristics of the floes shown in Figures 1 to 3 were: depth about 13 feet, width roughly 300 feet, and the velocity of flow varying between 0 and 2.3 fps depending on short term regulation of the power station.

The floes shown in Figures 4 to 6 formed on a channel with somewhat different characteristics: depth about 35 feet, width 200 feet, flow velocities varying between 0 and 4.0 fps, and a short-term regulated flow. Temperature measurements in this channel showed that the water temperature was constant at all depths, with a value of 0.01 C° measured at different locations along the channel.

To get an idea of the development of the surface configuration with time, an ice floe with a smooth upper side was turned and left in this

2. R. Beccat and B. Michel: International Association for Hydraulic Research, Proceedings 1959, Vol. III.

Fig. 1 — Ice floes from the Alvkarleby Head Race canal.

Fig. 2 — Ice floes from the Alvkarleby Head Race canal.

Fig. 3 — Ice floes from the Alvkarleby Head Race canal.

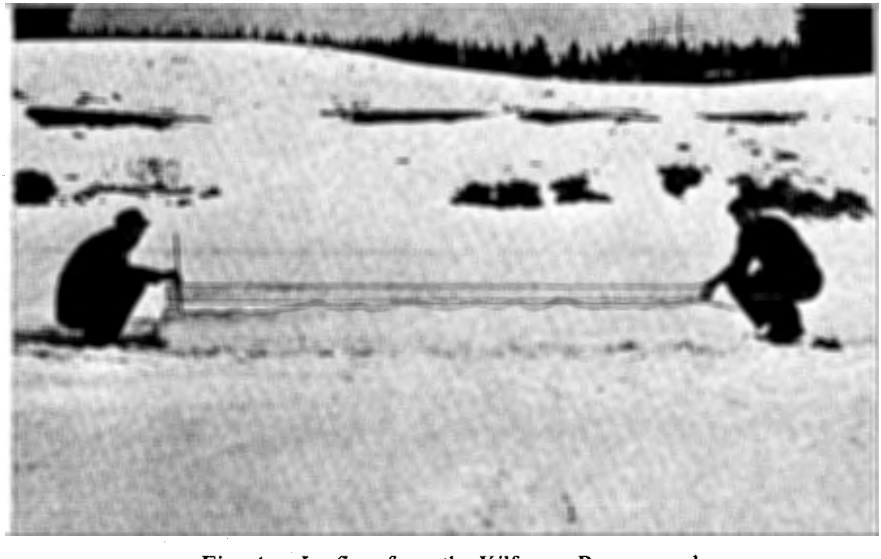

Fig. 4 — Ice floes from the Kilforsen Power canal.

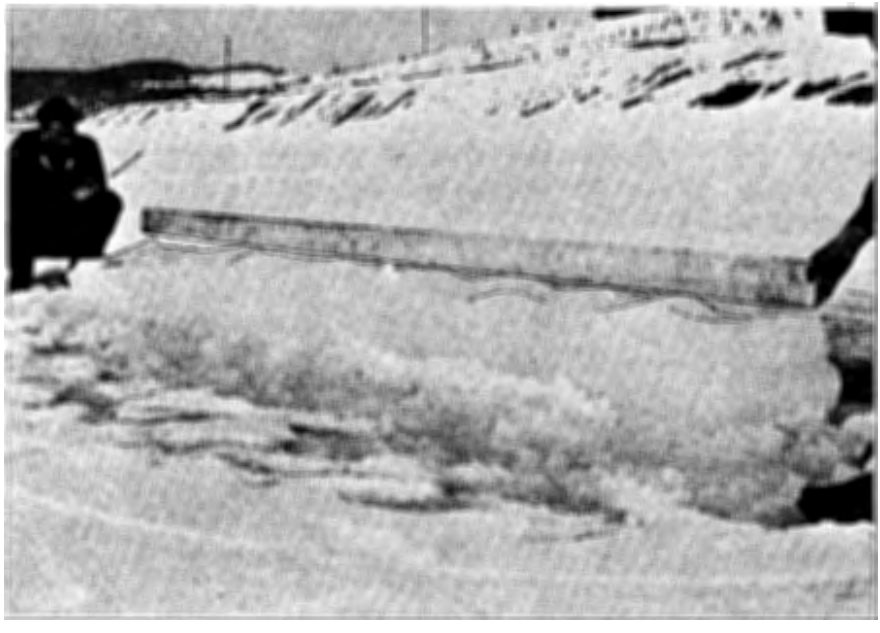

Fig. 5 — Ice floes from the Kilforsen Power canal.

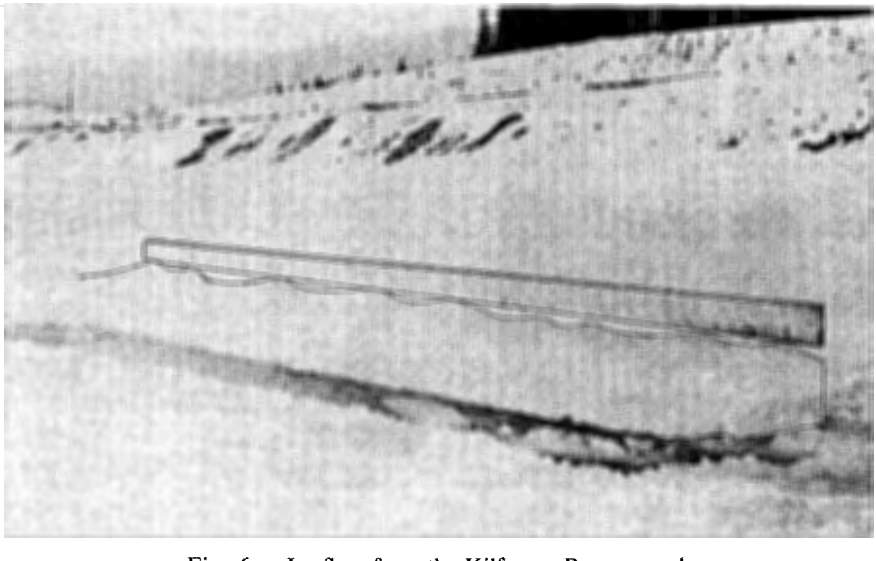

Fig. 6 — Ice floes from the Kilforsen Power canal.

position for 18 days. When turned again, the lower surface shown in Figure 7 had developed a pattern similar to that shown on Figure 2, although the amplitude of the waviness was considerably less. At the same time a new floe was cut and turned, downstream of the above-mentioned. Inspection showed that the surface configuration was similar to that observed 18 days earlier at the upstream floe. During the 18 days the air temperature was low with night temperatures of $-20°C$ and day temperatures from -7 to $-10°C$.

It is commonly assumed that ice with uneven thickness will rapidly become smooth. This is explained in the following way:

At locations with thin ice, the heat transfer would occur at a more rapid rate than at locations with thicker ice, thus resulting in a faster increase of the ice thickness in thin areas than in thick. This is assuming that the air temperature is below the freezing point. Figures 1 to 7 show that this theory does not hold. It appears that any attempt to mathematically describe the heat balance and ice production has to take into account some dynamic properties of the water flow. In connection with this, it is of interest to note the similarity between Figure 7 and Figure 8 which shows "ripples" produced by wind-transported snow. The resemblance to the waviness developed in an erodible channel is also apparent. It seems probable that the same mechanism is responsible for these different phenomena, a mechanism that is not completely understood. It also appears that experiments with flow under an ice cover could contribute to a better understanding of this property of turbulent flow.

Field observations have shown that the ice boundary is not a hydraulically smooth surface. With this in mind, the next step is to evaluate the hydraulic influence of the ice cover.

Hydraulic characteristics of an ice covered channel

From a hydraulic point of view, the ice covering of an open channel causes a radical change of conditions. The ice cover produces a substantial increase of the wetted perimeter, see Figure 9. For a wide channel the hydraulic radius is reduced to near half the value of the open channel radius, assuming a thin cover. The open channel is thus changed to a closed conduit but with the important difference that the cross sectional area will adjust according to the need because the ice is floating on the water surface.

To illustrate the effect of the reduction of the hydraulic radius, assume that the ice roughness is equal to the bottom roughness. If the thickness of the ice cover is assumed to be small, the hydraulic radius is reduced by a

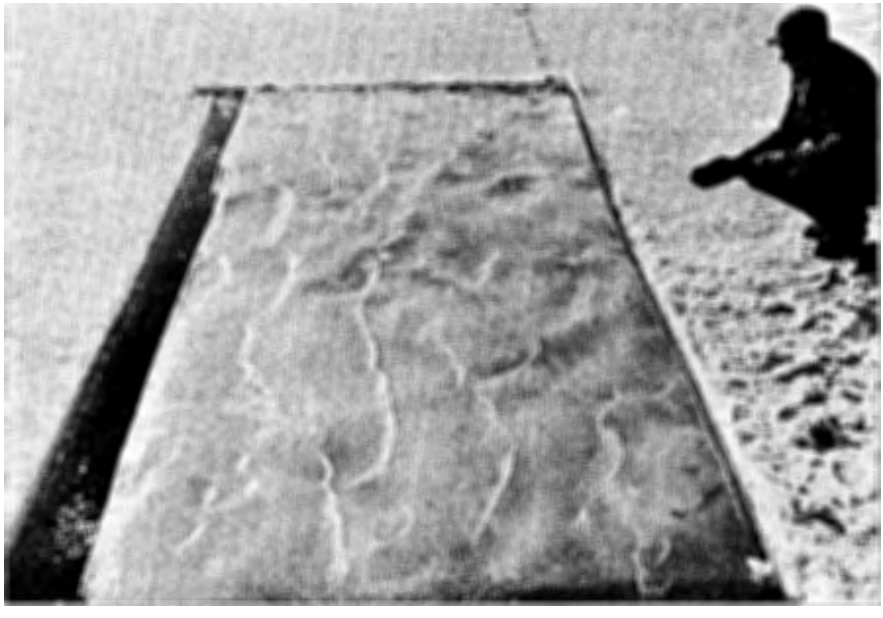

Fig. 7 — An originally smooth ice surface exposed to flow for 18 days.

Fig. 8 — Wind-blown snow.

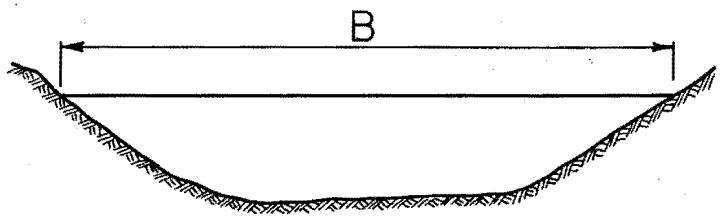

HYDRAULIC RADIUS

OPEN CHANNEL $R = \frac{A}{P}$

ICE COVERED $R = \frac{A}{P+B}$

Fig. 9 — Hydraulic radius for open — and ice covered cross section.

factor 2; and if the flow is kept constant, the head loss computed by the Manning equation is 2.5 times the head loss of the open channel.

The assumption of the ice roughness being equal to the roughness of the channel bottom is arbitrary and would, in general, not apply. For the usual case of the two boundaries with different roughness characteristics, a computation based on composite roughness would have to be applied to determine the head losses.

Formula for an equivalent roughness factor.

There are numerous formulas for computing the equivalent roughness factor of a cross section for which the roughness varies from part to part of the wetted perimeter. The cross section is divided into arbitrary subareas, according to the roughness prevailing in each part of the wetted perimeter. To derive an equivalent roughness factor applicable to the whole cross section, one of the following assumptions is generally applied:

1. The mean velocity of each of the subareas is equal to the mean velocity of whole cross section.
2. The resistance to flow of the whole cross section is equal to the sum of the resistances of the subareas.
3. The total discharge of the cross section equals the sum of the discharges of the subareas.

The common procedure in these assumptions is the subdivision of the cross sectional area. In order to derive a correct description of the physical behavior, the sub-areas should be chosen so that the flow within each area is governed by the type of roughness characteristic of the wetted perimeter assigned to that area. It is obvious that condition one above can be true only if the roughness is constant along the entire perimeter. Since the velocity distribution, and hence the mean velocity, are functions of the roughness, the mean velocities of areas with different roughnesses must be different. Condition two, however, is physically correct, provided the subdivision is correct. Condition three is true regardless of the subdivision because it involves only the continuity principle.

A formula which does not suffer any of the shortcomings mentioned, can be derived from the equations for velocity distribution in combination with the continuity equation. In the following derivation, the Manning formula is used for computing the energy loss. It is assumed that the relationship between the roughness height k and the Manning roughness coefficient can be expressed as:

$$n = ck^{1/6} \tag{1}$$

where c = 0.0316 according to C.F. Colebrook.[3] For laboratory use the derivation could as well be based on the Darcy-Weisbach friction factor f, thus eliminating the approximation involved in the above equation. It is further assumed that the flow is rough turbulent, a necessary condition for the validity of the Manning formula.

Let y_t be the total depth of flow in the ice covered channel, see Figure 10. The roughness heights are k_1 and k_2 for the ice cover and for the channel bottom respectively. The velocity distributions near the boundaries are governed by the roughness and the distance to the boundary according to the Prandtl-Karman velocity distribution law. At a particular distance from the boundaries, a maximum velocity occurs that is common to the two distributions. The shear, viscous as well as apparent, is zero at a horizontal plane through this elevation and thus, for uniform flow, this plane determines the subdivision in areas where the velocity distribution is governed by the ice roughness and the bottom roughness, respectively.

The velocity distribution for the upper region is:

$$v_1 = 2.5\, v_{f1} \ln \frac{30}{k_1} y \tag{2}$$

and for the lower region:

3. Colebrook, C. F.: The Flow of Water in Unlined, Lined and Partly Lined Rock Tunnels, 1958.

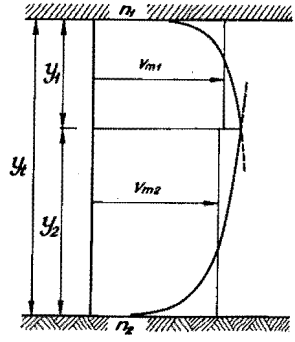

Fig. 10 — Theoretical velocity distribution. Definition sketch.

$$v_2 = 2.5\, v_{f2} \ln \frac{30}{k_2} y \tag{3}$$

where y is the distance from the respective boundaries.

The common maximum velocity occurs at the distances y_1 and y_2 from the ice cover and the channel bottom respectively: $(y_1 + y_2 = y_t)$.

$$v_{max} = 2.5\, v_{f1} \ln \frac{30}{k_1} y_1 = 2.5\, v_{f2} \ln \frac{30}{k_2} y_2$$

hence

$$\frac{v_{f1}}{v_{f2}} = \sqrt{\frac{\tau_1}{\tau_2}} = \frac{\ln \frac{30}{k_2} y_2}{\ln \frac{30}{k_1} y_1} = \frac{a}{b} \tag{4}$$

where the numerator is set equal to a and the denominator to b.

The mean velocities v_{m_1} and v_{m_2} are obtained by integration of the velocity functions and dividing by y_1 and y_2 respectively. The theoretical velocity is considered to be zero at the distance $\frac{k}{30}$ from the boundaries. The mean velocity for the upper region is:

$$v_{m1} = \frac{1}{y_1} 2.5\, v_{f1} \int_{\frac{k_1}{30}}^{y_1} \ln \frac{30}{k_1}\, y\, dy = \frac{1}{y_1} 2.5\, v_{f1} \left[y_1 \ln \frac{30}{k_1} y_1 - y_1 + \frac{k_1}{30} \right]$$

or

$$v_{m1} \cong 2.5\, v_{f1} \left(\ln \frac{30}{k_1} y_1 - 1 \right) \tag{5}$$

The term $\frac{1}{y_1} 25\, v_{f1} \frac{k_1}{30}$ is generally less than $10^{-3} v_m$ and is therefore considered to be negligible.

In the same manner, the mean velocity for the lower region is found:

$$v_{m2} \cong 2.5\, v_{f2} \left(\ln \frac{30}{k_2} y_2 - 1 \right) \tag{6}$$

Division of (5) by (6) and comparison with (4) yields:

$$\frac{v_{f1}}{v_{f2}} = \sqrt{\frac{\tau_1}{\tau_2}} = \frac{v_{m1}}{v_{m2}} \frac{\ln \frac{30}{k_2} y_2 - 1}{\ln \frac{30}{k_1} y_1 - 1} = \frac{v_{m1}}{v_{m2}} \left(\frac{a-1}{b-1} \right) \tag{7}$$

From the assumption of uniform flow it follows that the energy lines of the upper and the lower regions are parallel and also parallel to the energy line of the entire flow, i.e. $S_1 = S_2 = S$

The Manning formula applied to the upper and lower regions and to the whole cross section is:

$$v_{m1} = \frac{1.49}{n_1} y_1^{2/3} S^{1/2} \tag{8}$$

$$v_{m2} = \frac{1.49}{n_2} y_2^{2/3} S^{1/2} \tag{9}$$

$$v_m = \frac{1.49}{n} \left(y_{t/2} \right)^{2/3} S^{1/2} \tag{10}$$

Dividing (8) by (9) yields

$$\frac{v_{m1}}{v_{m2}} = \frac{n_2}{n_1}\left(\frac{y_1}{y_2}\right)^{2/3} \tag{11}$$

(11) combined with (7) and (4) gives:

$$\frac{y_1}{y_2} = \left(\frac{a(b-1)}{b(a-1)}\frac{n_1}{n_2}\right)^{3/2} \tag{12}$$

Finally, when the continuity equation,

$$y_1 v_{m1} + y_2 v_{m2} = y_t v_m \tag{13}$$

is combined with equations (8), (9) and (10) the following formula for the equivalent Manning coefficient is obtained:

$$\frac{1}{n} = \frac{\frac{1}{n_1} y_1^{5/3} + \frac{1}{n_2} y_2^{5/3}}{\left(\frac{1}{2}\right)^{2/3} y_t^{5/3}} \tag{14}$$

(When the metric system is used, M can be substituted for $\frac{1}{n}$)

This derivation was based on the assumption of a wide channel section where the influence of the side slopes is neglected. This assumption has not been introduced. It is, therefore, of interest to examine the equations further with respect to changes in depth. First, it is noted that the expression for the equivalent Manning coefficient can be written

$$\frac{1}{n} = \frac{(y_1/y_2)^{5/3}\frac{1}{n_1} + \frac{1}{n_2}}{\left(\frac{1}{2}\right)^{2/3}(y_1/y_2 + 1)^{5/3}} \tag{15}$$

which indicates, that $\frac{1}{n}$ is a function only of the ratio of y_1 to y_2 and thus independent of the total depth y_t . Next it is of interest to investigate the ratio $\frac{y_1}{y_2}$ with respect to y_t . Here it turns out that $\frac{y_1}{y_2}$ varies but slightly with the magnitude of y_t for the practical range of values of n_1 and n_2 . This is very important because it implies that it is possible to definitely compute the equivalent roughness factor for any given set of roughness coefficients n_1 and n_2 and thus to present a complete solution to the problem as a dimensionless plot. Figure 11 gives the ratio $\frac{n}{n_2}$ as a function of $\frac{n1}{n_2}$ in the range

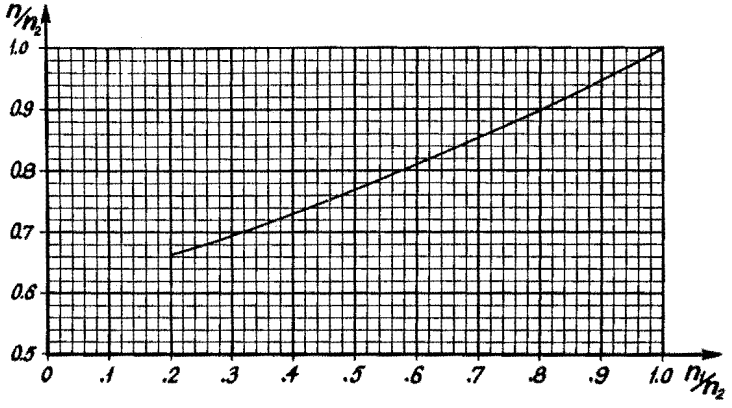

Fig. 11 — Composite roughness as a function of ice — and bottom roughness.

from 0.2 to 1.0, assuming $n_2 \leqq 0.04$ and $y_t \geqq 5$ feet. Here n_1 is the Manning n for the smoother of the two boundaries involved. Therefore the curve is valid also for the case where the ice roughness is greater than that of the channel bottom. In this case, obviously, the subscripts have to be interchanged.

It would appear that the expression for the equivalent roughness factor is valid for any cross sectional shape. This is, however, not true because the Prandtl-Karman law gives the velocity at a given point and for a given flow as a function of the wall roughness and the perpendicular distance from the point to the wall. Therefore, when a sloping portion of the cross section is considered, the distance to the plane of zero shear should be measured perpendicular to the slope.

If the total depth at a particular point is $y_t = y_1 + y_2$, the ratio of the distances determining the plane of zero shear is $\frac{y_1}{y_2 \cos \alpha}$ where α is the slope angle, see Figure 12. The error committed thus increases with the cosine of the angle, but for flat slopes is of minor importance.

With the composite Manning coefficient being determined according to the method indicated, head loss computations for the ice covered channel can be performed in the ordinary manner. The hydraulic radius is computed from $A/(P + B)$ where B is the width of the underside of the ice

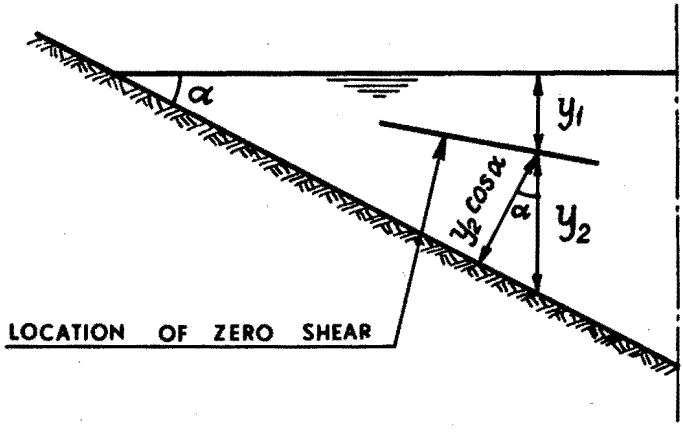

Fig. 12 — The effect of channel side slope. Definition sketch.

cover, and the cross sectional area A is corrected for the portion occupied by ice if the ice thickness is appreciable.

Determination of roughness from measured velocity distribution.

If the Prandtl-Karman equation for fully developed turbulence is assumed to be valid, the roughness of the boundary can be determined when the velocity distribution is known. Let y_0 be an arbitrary distance from the boundary. Equation (5) yields for the mean velocity:

$$v_m = 2.5\, v_f \left(\ln \frac{30}{k} y_0 - 1 \right) \tag{16}$$

The velocity at the distance y_0 from the boundary is determined from equation (2):

$$v_{max} = 2.5\, v_f \ln \frac{30}{k} y_0 = 2.5\, v_f\, a_1 \tag{17}$$

Division of equation (16) by equation (17) yields:

$$\frac{v_m}{v_{max}} = \frac{a_1 - 1}{a_1}$$

or

$$a_1 = \ln \frac{30}{k} y_0 = \frac{v_{max}}{v_{max} - v_m} = \frac{1}{1 - \frac{v_m}{v_{max}}}$$

from which $$k = 30\, y_0\, e^{-a_1} \tag{18}$$

The measured velocity distribution is plotted and the depth y_0 is chosen so that an accurate determination of a_1 is obtained. The mean velocity is determined and the roughness height then computed from equation (18). The Manning coefficient is finally computed from equation (1).

Determination of the roughness height can also be performed graphically by plotting the measured velocities on semilogarithmic paper where the measured velocities should fall on a straight line. This gives a convenient procedure for smoothing the measured values. The roughness height k is then found from the slope of the straight line as follows:

$$k = 30\, y^1 = 30 \times 10^{-\frac{v_{1.0}}{v_{1.0} - v_{0.1}}} \tag{19}$$

y^1 is the value of y for which the straight line intersects the velocity axis. $v_{1.0}$ and $v_{0.1}$ are the velocities at the distances 1.0 and 0.1 from the boundary, respectively.

Field Measurements

In order to obtain some information about actual ice roughness and about the increase of head losses due to an ice cover, a comprehensive field investigation was planned and performed by the Swedish State Power Board in 1960. The measurements were planned to be carried out on two occasions, one in summertime when the channel was open, and one in the wintertime with an ice cover on the channel. It was anticipated that the open channel measurements would give the roughness of the channel bottom, and the winter measurements would give the combined effect of ice roughness and the known bottom roughness. In addition, a comprehensive investigation of the velocity distribution close to the ice cover would yield information on the ice roughness.

The measurements were made in the supply channel of the Kilforsen Power Plant. Figure 13 gives a plan of the waterways adjacent to the power station. The water enters the head race from a pond approximately 17 miles long formed by damming the river Fjällsjöälven. The head race consists of a 6000-foot open channel, a 12,000-foot free-surface tunnel and a 2600-foot forebay. The station utilizes a head of close to 330 feet and discharges through a full-flowing tunnel about 9000 feet long. With a maximum flow of 13,200 cfs, the capacity is 340 MW from three units. As seen from the

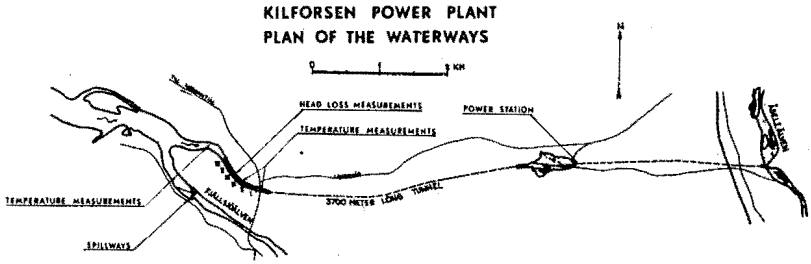

Fig. 13 — Plan of the Kilforsen Hydro Power Plant.

figures given, the plant is well adapted for the purpose of frequency and peak demand regulation which is generally performed by this station in coordination with other similar stations.

For the actual tests it was essential that the flow be kept constant during each test period. Therefore, the turbines were locked at a constant output during each run. The discharge was determined from the output, the over-all efficiency being known from recently-performed efficiency tests.

The winter measurements were carried out from February 23 to 26, 1960. The ice, at that time approximately 2 months old, was between 2 and 3 feet thick close to the channel banks, while the thickness on the main part of the channel varied between 4 and 8 inches.

A 2300-foot long section of the supply channel was chosen for the measurements, see Figure 14. Holes were drilled through the ice in six locations along this section, and steel poles were driven into the channel bottom. The elevation of the tops of the poles was determined by accurate leveling.

The velocity distribution was measured in four cross sections, see Figure 14. Holes were cut in these sections for insertion of the current meters. The meters had long tail fins and were suspended by wires because of the great depths. The holes, three feet long and 6 inches wide, were cut with the long direction perpendicular to the flow. Figure 15 shows examples of the velocity measurements, the crosses indicating the position of measuring points.

The velocity measurements were carried out by one crew at each cross section, and determined the duration of each test run. The time required was of the order of 3 hours, during which time the water surface elevation was measured every 5 minutes. The 2-to 3-foot deep holes served as stilling wells to produce a calm water surface, the elevation of which was measured with a ruler (1 mm divisions) from the top of the poles. The head between

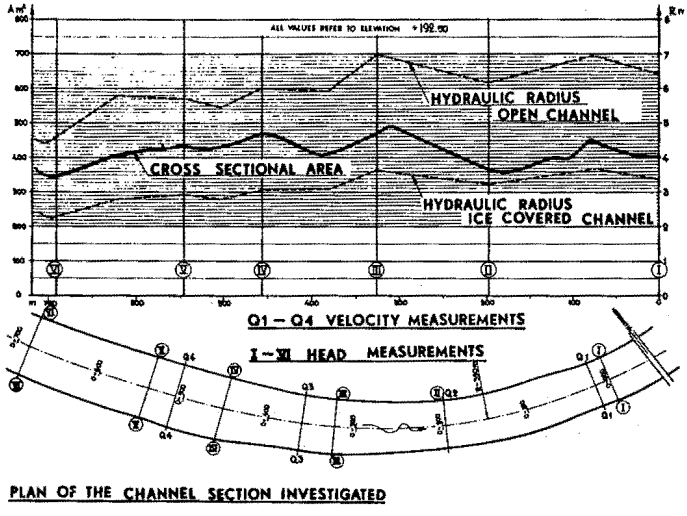

Fig. 14 — Plan of the investigated part of the power canal. Variation of cross sectional area and hydraulic radius.

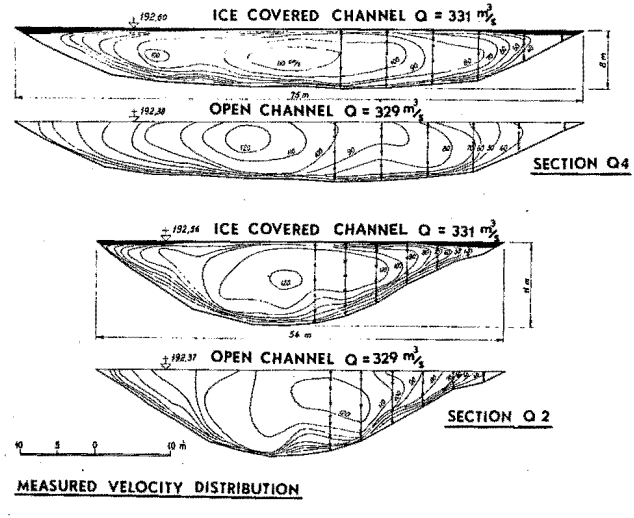

Fig. 15 — Velocity distribution in two cross sections. With and without ice.

the forebay and the draft tube exit, and the power output also, were measured every 5 minutes during each test. Measurements were performed with 4 different discharges in the range from 6100 cfs to 11,800 cfs.

The summer measurements, June 16-20, 1960, were performed in a similar way. Due to the smaller losses to be expected, a higher degree of accuracy was required. Accordingly, the water surface elevation was determined using point gages (1/10 mm reading) placed in stilling wells. The relative elevation of the point gages was established by hydrostatic leveling.

Velocity distribution was measured in two cross sections and at 4 different flows. Head losses were determined at 9 flows in the range from 5300 cfs to 12,400 cfs.

Wind velocities ranged between 0 and 9 fps, mainly in the direction of the channel flow, but did not affect the accuracy of the measurements.

During both summer and winter measurements, the flows into the Kilforsen reservoir were regulated to maintain the test flows in order to minimize variations in reservoir and channel surface elevation. Sufficient time was allowed prior to each test to reach a steady state condition.

During the summer measurements the channel reach was sounded at 9 cross sections. Since it was found that the cross sectional area was rather variable, see Figure 14, complementary soundings were made later. Thirty-eight new cross sections were introduced reducing the distance between successive cross sections to 65 feet. Figure 16 shows 6 typical cross sections.

Treatment of the Data Collected

The data obtained from the field measurements consisted of water surface elevations at six sections along the channel, at the power station intakes, and at the draft tubes, and of power output from the plant. The head losses in the supply tunnel were also measured to determine the roughness of the tunnel.[4] All of the data mentioned were time correlated. The water surface elevations were plotted as functions of time for each flow rate investigated. For each test period, a time interval was chosen within which the fluctuation of the surface elevations showed a minimum, and the average elevation was determined for this interval. This was done for each of the above-mentioned sections. Thus the result was an accurate water surface profile for each flow, and an accurate head at the power station. Accuracy determination based on the gathered data indicated a standard deviation of

4. See ASCE, Journal of the Hydraulics Division, HY4, July 1966: Factors Influencing Flow in Large Conduits, discussion by S. Angelin and Peter Larsen.

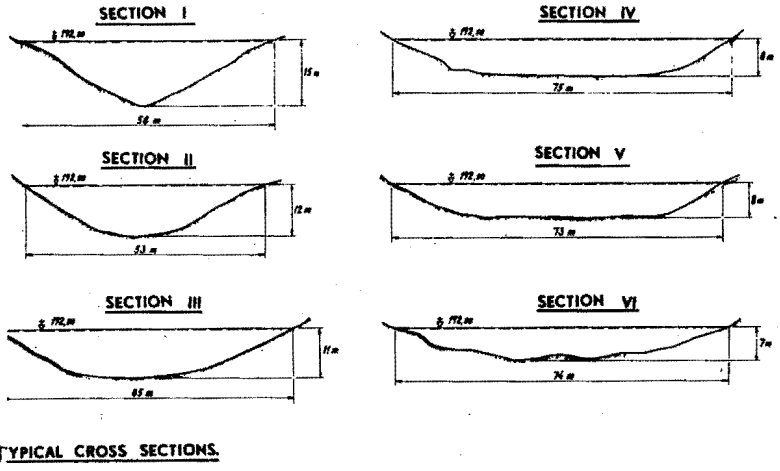

Fig. 16 — Typical cross sections.

0.7 and 0.5 mm in the water surface elevation of a section, for the winter and summer conditions respectively. The standard deviation for the difference in elevation of the water surface at the ends of the 2300-foot test reach was found to be 2.2 mm and 0.5 mm for the winter and summer conditions respectively.

The flow rate determined from the power output and the measured head were believed to run within 1% of the actual value for all tests.

The water surface profiles obtained for various flow rates were used, together with the soundings from 38 cross sections, as a basis for backwater computations. Since the Manning "n" was the unknown, it was varied in order to obtain the best agreement between measured and computed water surface profiles.

To obtain a comparison between the head losses for the open channel and those for the ice covered channel, all measurement results had to be converted to a common stage. Since the differences in stages at different tests were small ($\pm$ 0.7 feet from the chosen reference stage), the corrections needed to take into account only changes in cross sectional area, the changes in wetted perimeter being insignificant.

The velocity distribution measurements were treated according to the theoretical approach. Figure 17 shows the velocity distribution on a vertical measured at 4 diferent flows, and the computations based on these data. This was done for 40 verticals yielding 160 determined k values, the average of which was used for computation of the Manning "n" according to equation (1).

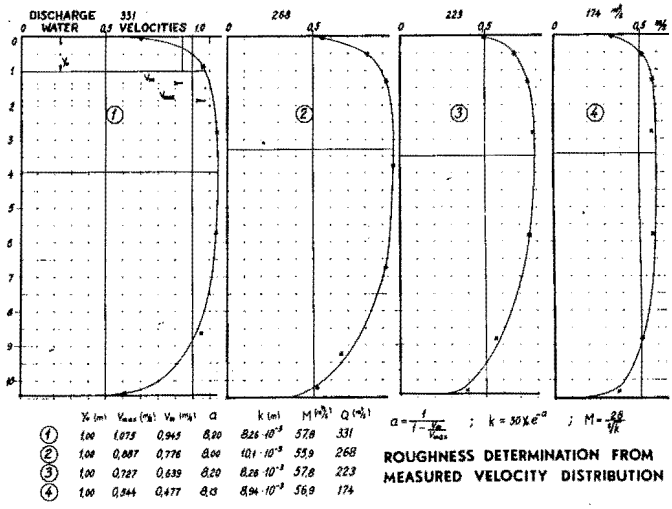

Fig. 17 — Vertical velocity distribution with 4 different flow rates.

Measurement Results

The results of the measurements made it possible to compare the composite roughness of the channel obtained in two different ways. The head loss computations gave n = 0.0333 for the open channel. This value of the Manning coefficient fitted all measured surface profiles equally well. An example of the measured and computed water surface profiles is given in Figure 18.

For the ice covered channel, it was similarly found from the head loss computations that n = 0.0270. Figure 19 shows an example of measured and computed surface profiles for the ice covered channel. Based on accuracy estimates it was concluded that:

Manning coefficient for the open channel, n = 0.0333 ± 0.0003

Manning coefficient for the composite roughness, n = 0.0270 ± 0.0007

The roughness of the ice cover was determined from the measured velocity distribution close to the cover. It was found that the Manning coefficient for the ice cover, n = 0.0192. Entering the Manning n-values, found for the channel bottom and for the ice cover, into the formulas for composite roughness, or using the diagram Figure 11, it was found that the Manning coefficient for the composite roughness n = 0.0267.

This result compared closely with the value determined by direct measurements.

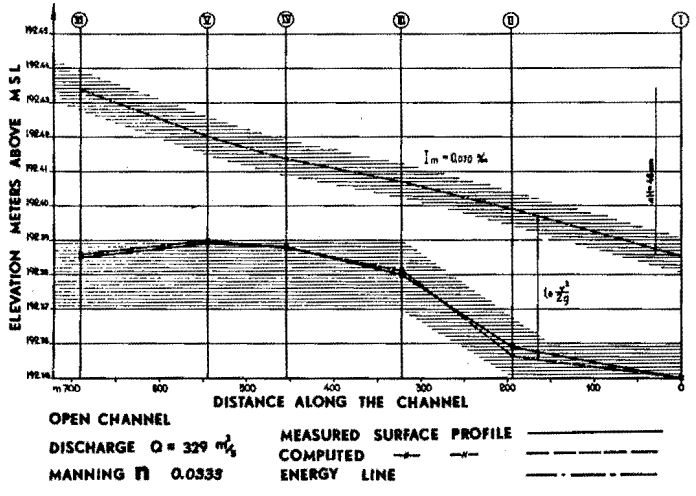

Fig. 18 — Computed and measured water surface profile without ice.

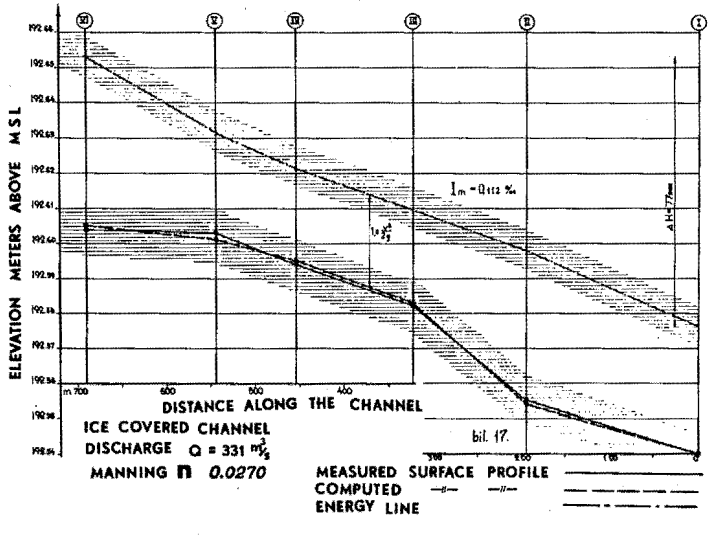

Fig. 19 — Computed and measured water surface profile with an ice cover.

The Manning coefficient for the open channel is high. This can be explained by the fact that the major part of the channel reach investigated is lined with a loose rip-rap protection consisting of bed rock material from the blasted supply tunnel.

It should be noted that the values of roughness height, computed primarily from the plotted velocity profiles, showed rather great fluctuations. This would, to some degree, be expected because the roughness varies from place to place, as seen from the photographs, Figures 1 to 6.

The head losses, referred to a common stage, are shown on Figure 20. The head losses with the ice cover was found to be 62% greater than the head losses of the open channel. It should be noted, however, that the channel investigated was rather rough, and that the head losses due to an ice cover could therefore be expected to amount to higher percentages of the open channel losses than those indicated above.

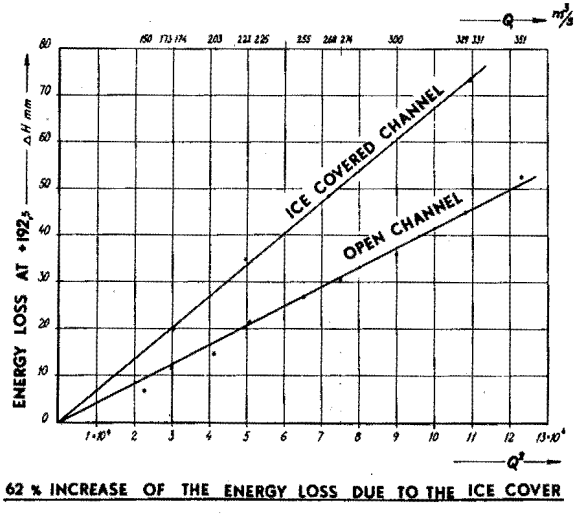

Fig. 20 — Head losses with and without an ice cover related to a common stage.

Concluding Remarks

The under surface of ice on a channel has been found to have irregularities that are formed by the flowing water. The effect of these irregularities corresponds to a certain roughness expressible in terms of an equivalent roughness height. The mechanics of the formation, however, are not known, and therefore it is not possible at the present time to predict the roughness of the ice cover on a channel of given hydraulic characteristics and given climatic conditions. Two lines of approach should be followed in order to adequately investigate the phenomena involved. The gathering of field data should continue, but this should be supplemented by systematic research and laboratory studies.

The formula derived for composite roughness is based on the assumption of two parallel (or slightly converging) boundaries, an assumption which merely limits the applicability to the case considered in this paper. The approach to the problem indicated herein, may be applicable to an attempt to develop a more general solution to the problem of composite roughness. The need for such a solution is obvious, both for design purposes and for laboratory use. Typical design problems include partly lined tunnels and channels with different construction materials used for bottom and side wall. A most significant example in the laboratory is in connection with flume tests conducted to evaluate the properties of various types of roughness. Numerous tests of this type have been performed in either relatively wide flumes, where the effect of the side walls has been disregarded, or in approximately square-shaped flumes with smooth sidewalls, the influence of which has been evaluated by some of the common formulas.